



## ORIGINAL ARTICLE

# Bizarre giant cells in human angiosarcoma exhibit chemoresistance and contribute to poor survival outcomes

Grace Fangmin Tan<sup>1</sup>  | Shane Goh<sup>2</sup> | Abner Herbert Lim<sup>2</sup> | Wei Liu<sup>2</sup> | Jing Yi Lee<sup>2</sup> | Vikneswari Rajasegaran<sup>2</sup> | Xin Xiu Sam<sup>3</sup> | Timothy Kwang Yong Tay<sup>3</sup> | Sathiyamoorthy Selvarajan<sup>3</sup> | Cedric Chuan-Young Ng<sup>2</sup> | Bin Tean Teh<sup>4,5,6,7,8</sup> | Jason Yongsheng Chan<sup>1,7,8</sup> 

<sup>1</sup>Division of Medical Oncology, National Cancer Centre Singapore, Singapore City, Singapore

<sup>2</sup>Integrated Genomics Platform, National Cancer Centre Singapore, Singapore City, Singapore

<sup>3</sup>Department of Anatomical Pathology, Singapore General Hospital, Singapore City, Singapore

<sup>4</sup>Laboratory of Cancer Epigenome, National Cancer Centre Singapore, Singapore City, Singapore

<sup>5</sup>Program in Cancer and Stem Cell Biology, Duke-NUS Medical School, Singapore City, Singapore

<sup>6</sup>Institute of Molecular and Cell Biology, Singapore City, Singapore

<sup>7</sup>Cancer Science Institute of Singapore, National University of Singapore, Singapore City, Singapore

<sup>8</sup>Oncology Academic Clinical Program, Duke-NUS Medical School, Singapore City, Singapore

## Correspondence

Jason Yongsheng Chan, Division of Medical Oncology, National Cancer Centre Singapore, Singapore City, Singapore.  
Email: jason.chan.y.s@nccs.com.sg

## Funding information

Singapore Ministry of Health's National Medical Research Council of Singapore, Grant/Award Number: NMRC/FLWSHP/054/2017-00, NMRC/CG/C012B/2017\_NCCS, MOH-STAR18NOV-0001; SHF-Foundation, Grant/Award Number: SHF/FG653P/2017; SingHealth Duke-NUS Academic Medical Centre and Oncology ACP, Grant/Award Number: 08-FY2017/P1/14-A28

## Abstract

Giant cells (GC) are a poorly understood subset of tumor cells that have been increasingly recognized as a potential contributor to tumor heterogeneity and treatment resistance. We aimed to characterize the biological and clinical significance of GC in angiosarcoma, an aggressive rare cancer of endothelial origin. Archival angiosarcoma samples were examined for the presence of GC and compared with clinicopathological as well as NanoString gene expression data. GC were examined in angiosarcoma cell lines MOLAS and ISOHAS using conventional and electron microscopy, single cell whole genome profiling, and other assays. In the cell lines, GC represented a rare population of mitotically active, non-senescent CD31<sup>+</sup> cells, and shared similar genomic profiles with regular-sized cells, consistent with a malignant endothelial phenotype. GC remained viable and persisted in culture following exposure to paclitaxel and doxorubicin. In patient samples, GC were present in 24 of 58 (41.4%) cases. GC was correlated with poorer responses to chemotherapy (25.0% vs 73.3%,  $P = 0.0213$ ) and independently contributed to worse overall survival outcomes (hazard ratio 2.20, 95% confidence interval 1.17-4.15,  $P = 0.0142$ ). NanoString profiling revealed overexpression of genes, including *COL11A1*, *STC1*, and *ERO1A*, accompanied by upregulation of immune-related metabolic stress and metastasis/matrix remodeling pathways in GC-containing tumors. In conclusion, GC may contribute to chemoresistance and poor prognosis in angiosarcoma.

## KEYWORDS

angiosarcoma, chemoresistance, prognosis, rare cancer, sarcoma

This is an open access article under the terms of the Creative Commons Attribution-NonCommercial License, which permits use, distribution and reproduction in any medium, provided the original work is properly cited and is not used for commercial purposes.

© 2020 The Authors. *Cancer Science* published by John Wiley & Sons Australia, Ltd on behalf of Japanese Cancer Association.

## 1 | INTRODUCTION

Bizarre giant cells (GC) are enlarged cells that are often multinucleated. They are alternatively referred to as polyploid giant cancer cells (PGCC) or “monster” cells in some studies, among a wide-ranging nomenclature.<sup>1</sup> They have been recognized in various malignancies, including those of the colorectum,<sup>2</sup> ovary,<sup>3,4</sup> breast,<sup>5,6</sup> and prostate,<sup>7</sup> as well as in soft tissue tumors.<sup>8</sup> Despite their ubiquity, GC are poorly characterized, especially in sarcomas, and their clinical and biological relevance are not well studied. Some authors regard GC as polyploid cells in mitotic catastrophe generated via endoreplication,<sup>9</sup> previously thought to be senescent. Recent studies have demonstrated that such GC are metabolically active and may contribute to tumor heterogeneity and treatment resistance.<sup>6</sup> Despite their often multinucleate nature, it has been demonstrated that GC are able to give rise to viable, tumorigenic progeny via various depolyploidization mechanisms, such as budding and bursting.<sup>2</sup> Conversely, GC in some tumor types, such as Wilm’s tumor, represent anaplastic/pleomorphic cells in which mitoses can be expected to occur.<sup>10</sup> To resolve the uncertainty, we decided to study the nature and significance of GC in angiosarcoma in greater detail.

Angiosarcomas are a rare, aggressive subtype of soft tissue sarcomas of endothelial cell origin.<sup>11–13</sup> These tumors often demonstrate significant heterogeneity in terms of clinical presentation and can arise in several anatomical regions, including the head and neck, breast, viscera, trunk, and extremities. Furthermore, angiosarcomas are notoriously challenging to treat and survival outcomes are disappointing despite multimodality strategies incorporating surgery, radiation therapy, and chemotherapy.<sup>13,14</sup> Notably, administration of chemotherapeutic agents, including paclitaxel, doxorubicin, or targeted agents, is typically met with short-lived responses and rapid development of drug resistance.<sup>15</sup> Apart from standard clinical indicators such as age, performance status, and stage of disease,<sup>16</sup> there is currently a lack of biomarkers to predict survival outcomes and chemotherapy response, the latter of which may be particularly useful to select patients for appropriate therapy.

Giant cells have been described in angiosarcomas and have been suggested to differentiate them from epithelioid hemangioendotheliomas.<sup>17,18</sup> There has been hitherto a lack of interest in characterizing these GC in angiosarcomas and understanding their clinical implications, although it may be speculated that these bizarre anaplastic cells represent an aggressive phenotype and may harbor chemoresistant properties.

Therefore, the present study seeks to provide an initial characterization of GC in angiosarcoma, as well as to examine their biological and clinical significance, integrating clinicopathological information, molecular profiling, and in vitro modeling.

## 2 | MATERIALS AND METHODS

### 2.1 | Study cohort

Patients with a diagnosis of angiosarcoma at the Singapore General Hospital and the National Cancer Centre Singapore from January

2000 to December 2018 were included in our study. Fifty-eight patients with angiosarcoma were selected on the basis of tissue availability. All samples were obtained following written informed consent in accordance with the Declaration of Helsinki. Participants and/or their legal guardians provided informed consent for their data to be used in this research. This study has been approved by the SingHealth Centralised Institutional Review Board (2010/426/B). All data were obtained at the time of diagnosis or subsequent follow up. The datasets created and analyzed in this study are available from the corresponding author upon reasonable request. The clinicopathological characteristics of all patients with angiosarcoma are summarized in Table 1.

### 2.2 | Microscopic examination of giant cells

Archival slides of H&E-stained, formalin-fixed paraffin-embedded (FFPE) samples were obtained from the Department of Pathology, Singapore General Hospital. The FFPE samples included both small core biopsy ( $n = 9$ ) and surgical biopsy specimens ( $n = 49$ ), of which one representative slide from each patient was examined. Only samples with adequate tissue were included, and at least 10 high power fields could be examined. One representative tumor section was examined for each patient’s primary tumor sample and evaluated for the presence of GC through microscopic examination at 100 $\times$  and 400 $\times$  magnification. GC were defined as atypical large cells harboring either (a) multiple nuclei or (b) bizarre hyperchromatic nuclei with more than threefold the diameter of nuclei in surrounding angiosarcoma cells, in keeping with previous published literature.<sup>1,3,5,7</sup> Histological features were also recorded, including mitotic count, and the presence of necrosis and epithelioid components. Tumors were graded as low, intermediate, or high with reference to the FNCLCC system.<sup>19</sup>

### 2.3 | Cell lines and cell viability assays

Two angiosarcoma cell lines (MOLAS and ISOHAS) were obtained from the Cell Resource Center for Biomedical Research, Institute of Development, Aging and Cancer, Tohoku University, Japan, courtesy of Dr Mikio Masuzawa. MOLAS was established from a patient with scalp lymphangiosarcoma metastatic to the pleura, while ISOHAS was established from a patient with primary scalp hemangiosarcoma. Both cell lines were maintained in DMEM medium supplemented with 10% FBS and 1% penicillin/streptomycin. These cells were grown in a humidified chamber with 5% CO<sub>2</sub> at 37°C and examined in situ under bright-field microscopy for morphology and presence of GC. To examine the response to chemotherapeutic agents, MOLAS and ISOHAS cultures were exposed to paclitaxel and doxorubicin (Abcam) at concentrations of 5, 10, 25, and 50 ng/mL for 120 hours. The trypan blue assay was used to assess the overall cell viability after treatment with the respective agents. Cell cultures at approximately 70% confluence were used for all experimental drug treatments unless otherwise stated.

**TABLE 1** Clinicopathological features and presence of giant cells

Characteristic (n)	Giant cells in primary tumor sample		P
	Present (%)	Absent (%)	
Total (58)	24 (41.4)	34 (58.6)	—
Sex			
Male (34)	21 (61.8)	13 (38.2)	.0015
Female (24)	3 (12.5)	21 (87.5)	
Age			
>65 y (26)	13 (50.0)	13 (50.0)	n.s.
≤65 y (32)	11 (34.4)	21 (65.6)	
Ethnicity			
Chinese (50)	22 (44.0)	28 (56.0)	n.s.
Non-Chinese (8)	2 (25.0)	6 (75.0)	
Tumor location			
Skin (29)	13 (44.8)	16 (55.2)	n.s.
Other (29)	11 (37.9)	18 (62.1)	
ECOG performance status			
0 (35)	13 (37.1)	22 (62.9)	n.s.
≥1 (23)	11 (47.8)	12 (52.2)	
Known risk factors			
No (44)	23 (52.3)	21 (47.7)	n.s.
Yes (14)	1 (7.1)	13 (92.9)	
Metastasis at diagnosis			
Absent (40)	18 (45.0)	22 (55.0)	n.s.
Present (18)	6 (33.3)	12 (66.7)	
Tumor grade			
Low (15)	4 (26.7)	11 (73.3)	n.s.
Intermediate (20)	8 (40.0)	12 (60.0)	
High (23)	12 (52.2)	11 (47.8)	
Mitotic score			
Low (33)	8 (24.2)	25 (75.8)	.0437
Intermediate (9)	5 (55.6)	4 (44.4)	
High (16)	11 (68.8)	5 (31.2)	
Tumor necrosis			
None (35)	11 (31.4)	24 (68.6)	n.s.
<50% (11)	7 (63.6)	4 (36.4)	
≥50% (12)	6 (50.0)	6 (50.0)	
Epithelioid component			
Absent (24)	8 (33.3)	16 (66.7)	n.s.
Present (34)	16 (47.1)	18 (52.9)	

n.s., non-significant.

## 2.4 | CD31 immunohistochemistry

Sections (4 μm) were cut from FFPE tissue blocks, mounted onto positively charged Bond Plus Slides (Leica Biosystems), and dried on a heating bench for at least 20 minutes. After deparaffinization and

rehydration, tissue samples were subjected to high temperature-induced epitope retrieval through 5 minutes of pressurized heating at 120°C in a T/T mega microwave (Milestone). The sections were then performed on Dako Autostainer Plus (Dako). Endogenous peroxidase activity was blocked using hydrogen peroxide (Dako S2022) for 10 minutes. Primary antibody against CD31 was diluted in antibody diluent with background-reducing components (Dako) at a dilution of 1:400. Slides were incubated with the respective optimized primary antibody for 30 minutes at room temperature. The detection system used was the Dako Envision Detection Kit (K5007), which consists of a dextran backbone conjugated with secondary antibodies to mouse immunoglobulin and HRP. Addition of the substrate chromogen diaminobenzidine for 5 minutes produced an insoluble brown precipitate, as catalyzed by HRP. Slides were removed from the Autostainer and counterstained with Mayer's Hematoxylin (Dako S3309). Appropriate controls were run with each batch of slides. CD31 staining was demonstrated in vascular endothelial cells using normal colonic tissue as positive control. Negative controls consisted of the omission of primary antibody without any other changes to subsequent procedures.

## 2.5 | Transmission electron microscopy

Angiosarcoma cell lines MOLAS and ISOHAS were evaluated by transmission electron microscopy (TEM). Cell pellets were prepared and fixed using 1.6% glutaraldehyde and 2.5% paraformaldehyde in 0.1 mol/L sodium cacodylate buffer, pH 7.2-7.4 (Electron Microscopy Sciences), post-fixed in osmium tetroxide, stained en bloc in uranyl acetate, dehydrated in an ethanol series and propylene oxide, before being infiltrated to Araldite resin and polymerized. Semi-thin sections (1 μm) were cut and mounted on glass slides, stained with toluidine blue, and examined by light microscopy for general quality of fixation, gross cell morphology, and for the presence of mitotic cells and dead or dying cells. Ultra-thin sections (0.1 μm) were cut with an ultra-microtome and mounted on electron microscope grids. The sections were stained with uranyl acetate and lead citrate solutions. At least 100 cell profiles were examined (SGS Vitrology).

## 2.6 | Senescence assay

Identification of senescent cells was based on a histochemical stain for beta-galactosidase activity at pH 6 using the Senescence Cells Histochemical Staining Kit (Sigma) as per the manufacturer's protocol. The cell lines were grown in six-well plates, washed with PBS, and subsequently fixed at room temperature with 1× fixation buffer. Cells were incubated with staining mixture for 2 hours at 37°C without CO<sub>2</sub>. Mouse embryonic fibroblasts (MEF) containing senescent cells were used as positive controls. Senescent cells were stained blue, while the rest of the cells remained unstained.

## 2.7 | Gene expression analysis via Nanostring PanCancer IO 360 panel

We used the NanoString PanCancer IO360 panel (NanoString Technologies) to investigate gene expression on FFPE tissue as previously described,<sup>13</sup> following the manufacturer's protocol using the nCounter platform. RNA was extracted from five 10- $\mu$ m sections on all samples with adequate tumor tissue available and analyzed using the 2100 Bioanalyzer (Agilent Technologies). After excluding samples with suboptimal RNA integrity and content, the remaining samples were included in the nCounter analysis. The final set of data passing QC ( $n = 34$ ) were analyzed on the nSolver 4.0 Advanced Analysis module using the default settings to derive differentially expressed genes, pathway scores, and cell-type scores.

## 2.8 | DepArray single cell isolation and whole genome sequencing

The DEPAArray NxT system (Menarini Silicon Biosystems) was used to isolate the large cells prior to downstream analysis. Cells were fixed with paraformaldehyde followed by washing. Approximately 20 000 cells were loaded into the DEPAArray cartridge (Menarini Silicon Biosystems) for imaging. Cells were then sorted by size, and the largest 100 cells were visually inspected for overall integrity before being individually isolated. Average-sized cells were also isolated for comparative study. DNA isolation and whole genome amplification were performed using the Ampli1 WGA Kit (Menarini Silicon Biosystems) and checked for quality using the Ampli1 QC Kit. Only products with a genome integrity index (GII) of 4 were retained for low pass whole genome sequencing performed at 5 $\times$  coverage. The raw reads were then mapped using BWA,<sup>20</sup> duplicates removed, and base recalibrated before calling CNA using IchorCNA 0.2.0 with a 500-kb bin integral.<sup>21</sup> The plots below were then generated using an R package called "ComplexHeatmap."

## 2.9 | Statistical analyses

The presence of GC in primary tumor samples was compared against clinicopathological data, which included patient demographics, FNCLCC grading, Eastern Cooperative Oncology Group (ECOG) performance status, tumor characteristics, treatment response, and survival outcomes. To examine the potential of GC status for use in prognostication, we compared survival outcomes

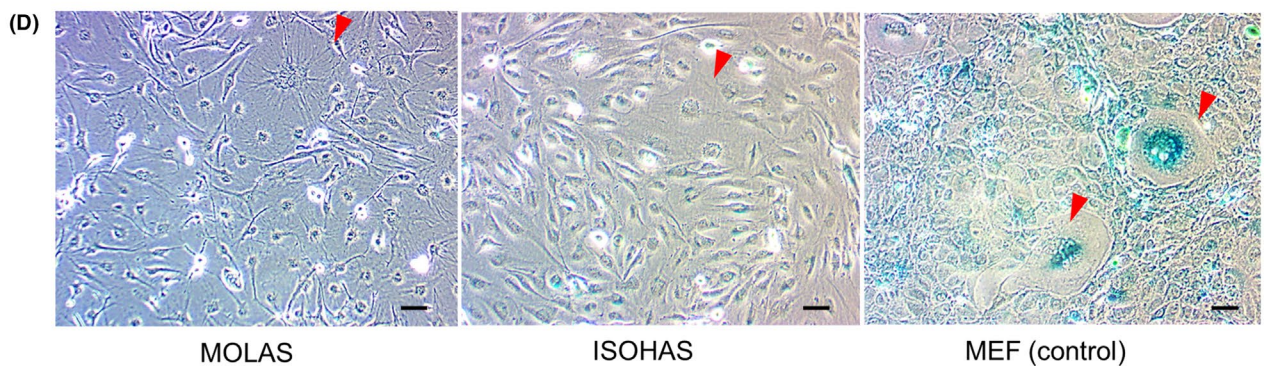
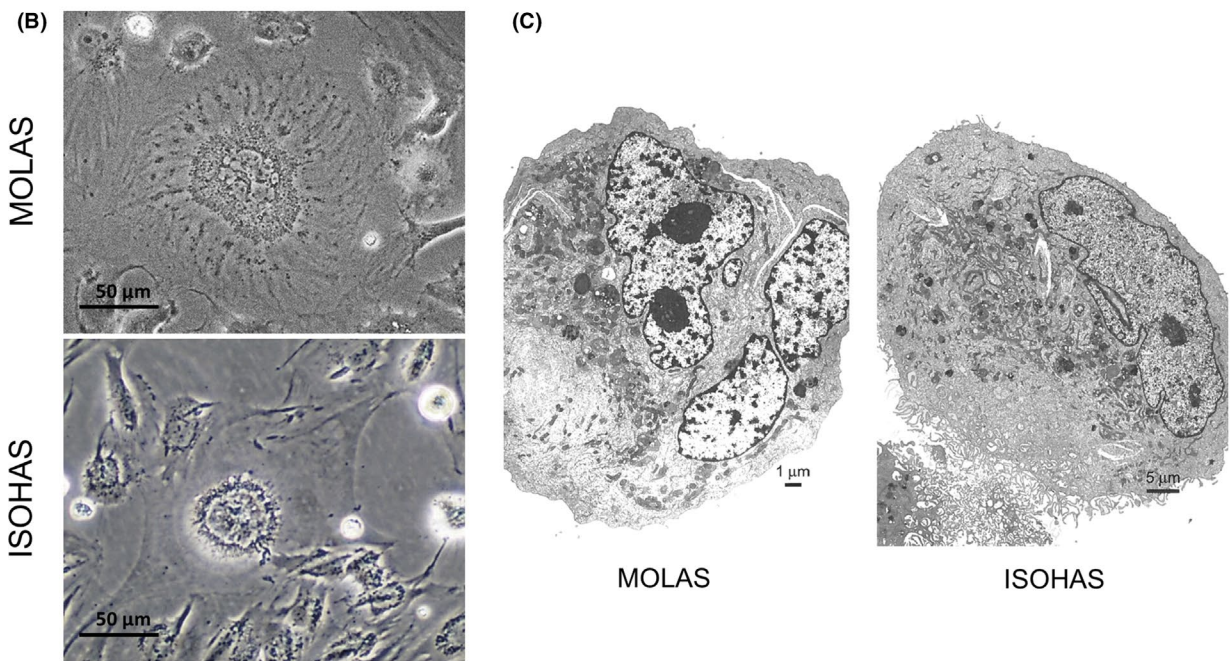
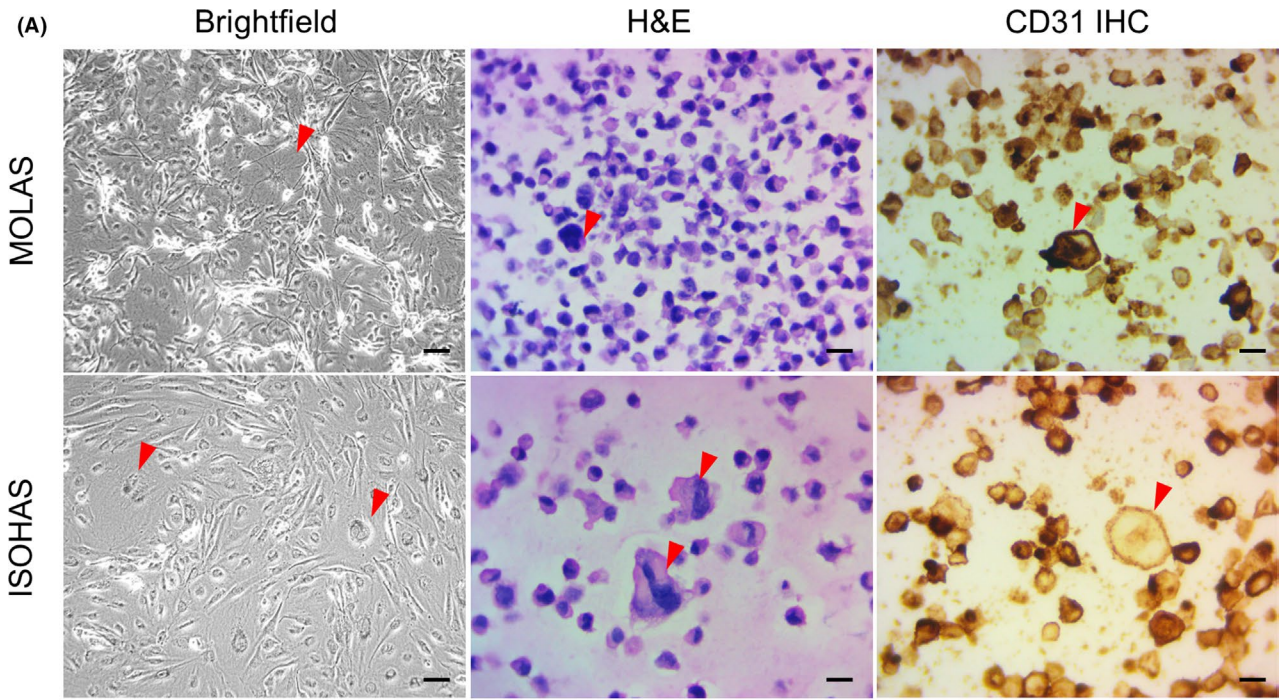
stratified by FNCLCC grade, as well as a modified FNCLCC grading system in which GC positivity was deemed a signature of high-grade disease. In our modified FNCLCC grading, tumor grade was first defined by conventional FNCLCC scoring, following which all GC-positive patients were upgraded to high-grade status. Objective treatment response was assessed using the Revised RECIST guidelines (version 1.1)<sup>22</sup> Overall survival (OS) was calculated from date of initial histological diagnosis to date of death from any cause, or was censored at the date of last follow up for survivors; cancer-specific survival (CSS) was calculated from date of initial histological diagnosis to date of death from angiosarcoma. Progression-free survival (PFS) was calculated from date of initial histological diagnosis to date of disease progression, or death from any cause. Survival analysis was performed using the Kaplan-Meier method and Cox proportional hazard models. Univariate and multivariate analyses of categorical variables were conducted using  $\chi^2$  and logistic regression tests, respectively. All analyses were conducted using MedCalc, version 9.6.2.0., and the threshold for statistical significance was taken as two-tailed  $P < 0.05$  for all analyses.

## 3 | RESULTS

### 3.1 | Characterization of giant cells in angiosarcoma cell lines

Examination of MOLAS and ISOHAS cell lines revealed GC in both cell populations. GC observed under brightfield microscopy were large, atypical cells with multiple or single enlarged nuclei. GC observed in H&E-stained MOLAS and ISOHAS cells similarly demonstrated large cells with multiple or enlarged hyperchromatic nuclei, of which cellular and nuclear size exceeded three times that of surrounding regular angiosarcoma cells. (Figure 1A). GC stained positive for CD31, in keeping with their endothelial origin. Higher magnification revealed that these bizarre cells possess a flattened morphology reminiscent of senescent cells, with abnormal nuclei, and are typically surrounded by smaller, regular-sized cells (Figure 1B). TEM of GC in both cell lines revealed significant cellular and nuclear pleomorphism. These GC contained numerous mitochondria (sometimes swollen) and included cells in mitosis (Figure 1C). MOLAS and ISOHAS cell lines were examined for beta-galactosidase staining as a marker of cellular senescence. In both cell lines, however, the majority of GC were non-senescent. MEF cell lines used as positive controls showed appropriate blue staining of cells undergoing replicative senescence (Figure 1D).

**FIGURE 1** Giant cell (GC) in human primary angiosarcoma cell lines. A, GC (red arrowheads) in MOLAS and ISOHAS cell lines under brightfield microscopy, H&E staining, and CD31 immunohistochemistry. Membranous staining for CD31 is in keeping with their endothelial origin. B, GC at higher magnification. C, Electron microscopy of representative MOLAS and ISOHAS GC. GC demonstrated cellular and nuclear pleomorphism as well as numerous mitochondria. D, Senescence assay demonstrated that most GC in MOLAS and ISOHAS cell lines exhibit weak or absent staining compared to giant mouse embryonic fibroblast mouse embryonic fibroblasts cells undergoing replicative senescence (positive control) (scale bar, 20  $\mu$ m unless otherwise stated)



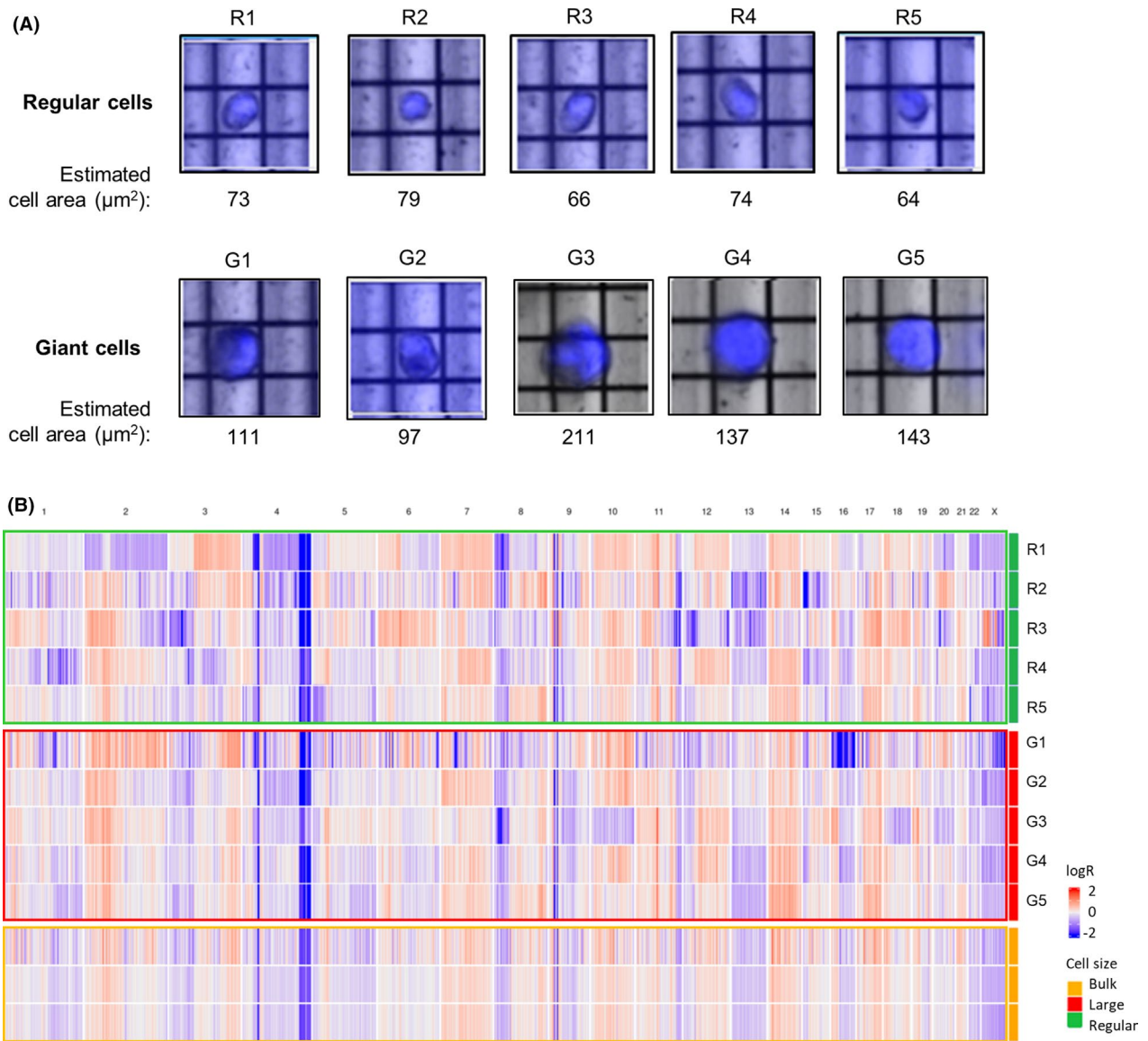


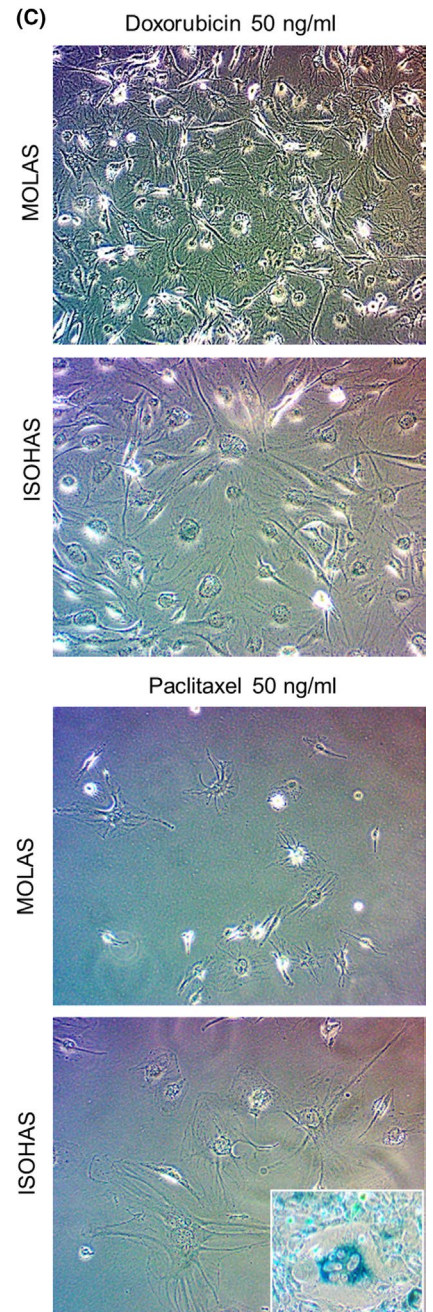
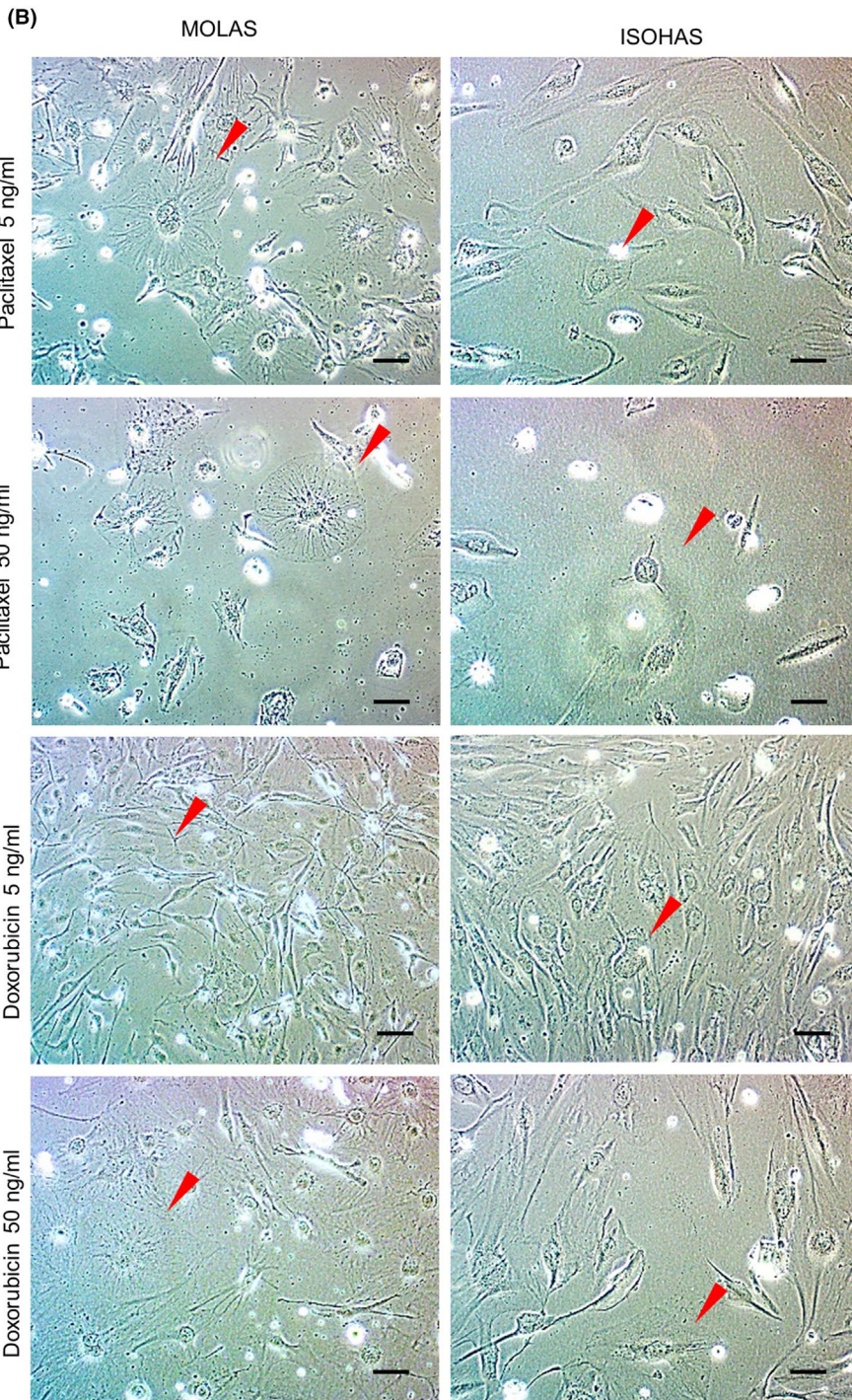
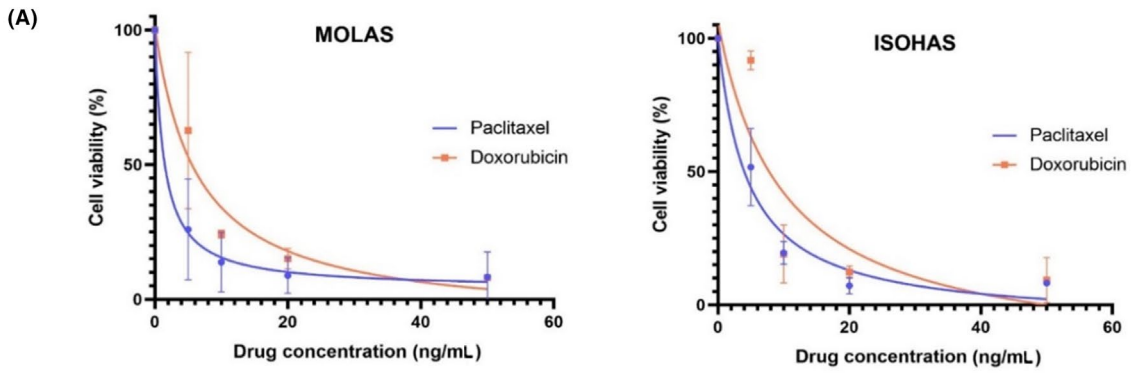
**FIGURE 2** Single cell whole genomic profiling of large and regular-sized cells within the MOLAS cell line. A, Visual inspection and isolation of giant cells and regular-sized cells. B, logR plots of large cells in comparison to regular cells and with cells sequenced in bulk demonstrated major similarities in their copy number landscapes, suggesting that large cells are of the same malignant origin as regular-sized cells

### 3.2 | Single cell whole genomic sequencing

To test whether GC are of the same malignant origin as the regular-sized cells, we performed single cell whole genomic profiling of large cells ( $n = 5$ ) and regular-sized cells ( $n = 5$ ) within the MOLAS cell line,

as well as cells sequenced in bulk ( $n = 3$ ). We demonstrated that large cells, in comparison to regular cells as well as with cells sequenced in bulk, shared major similarities in their copy number landscapes, suggesting that large cells carry the same genomic profiles as regular-sized cells (Figure 2).

**FIGURE 3** Persistence of giant cells (GC) in angiosarcoma cell lines after treatment with chemotherapy. A, Dose-response curves of paclitaxel and doxorubicin for MOLAS and ISOHAS cell lines. B, Brightfield microscopy of angiosarcoma cells exposed to varying concentrations of chemotherapeutic drugs revealed an increased proportion of GC (red arrowheads) post-treatment (scale bar, 20  $\mu\text{m}$ ). C, GC in MOLAS and ISOHAS cell lines that remained following exposure to doxorubicin or paclitaxel were non-senescent. Inset: Mouse embryonic fibroblasts cells undergoing replicative senescence (positive control) stained blue



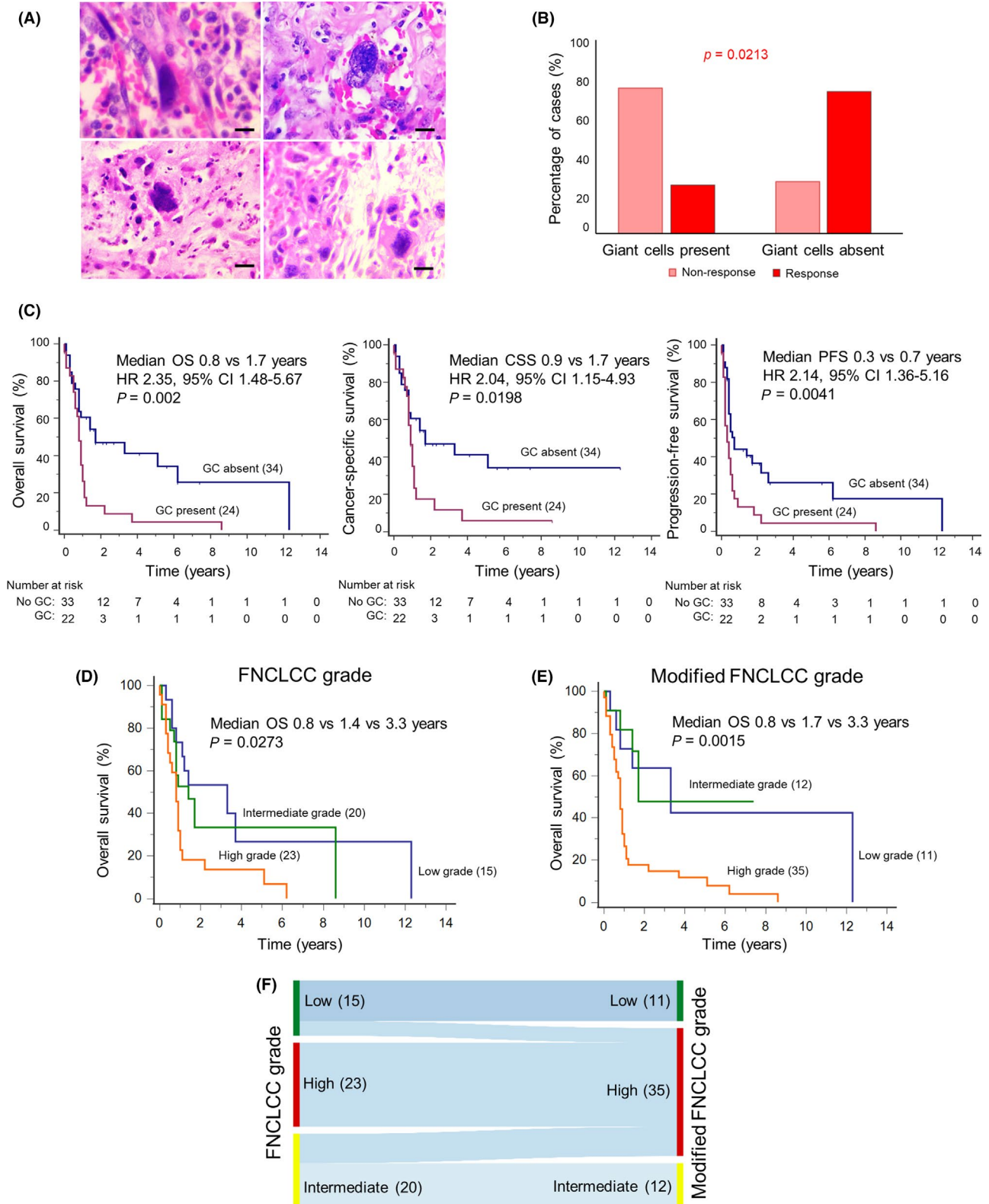


**FIGURE 4** Giant cell (GC) in human primary angiosarcoma. A, GC visible in H&E-stained angiosarcoma primary tumor samples. B, Compared to those without GC, the presence of GC was associated with a lower rate of objective response (25.0% vs 73.3%,  $P = .0213$ ) to chemotherapy. C, Presence of GC was independently associated with inferior survival outcomes. D, Higher FNCLCC grading was associated with poorer survival outcomes. E, Integrating GC presence as a high-grade feature to form a modified FNCLCC score further improved stratification of survival outcomes. F, A Sankey plot illustrates the reclassification of some FNCLCC low and intermediate grade tumors to high grade based on presence of GC. CI, confidence interval; CSS, cancer-specific survival; OS, overall survival; PFS, progression-free survival



### 3.3 | In vitro response to chemotherapeutic drugs

MOLAS and ISOHAS cell lines were exposed to increasing concentrations of paclitaxel and doxorubicin (5, 10, 25, and 50 ng/mL for 120 hours). Both drugs resulted in a dose-dependent reduction in cell viability in the angiosarcoma cell lines (Figure 3A). Inspection of treated cell lines showed that GC remained in culture despite exposure to increasing drug concentrations. At 50 ng/mL, GC were the dominant cell population in culture and few non-GC remained at the end of 120 hours (Figure 3B). GC in MOLAS and ISOHAS cell lines that remained following exposure to doxorubicin or paclitaxel were non-senescent and persisted in culture (Figure 3C).

### 3.4 | Correlation of giant cells with clinical characteristics

We examined clinical specimens of primary angiosarcoma samples for the presence of GC. In the study cohort, the median age at diagnosis was 63 years (range: 32-88), and male patients accounted for 58.6% of the cases. The most common primary tumor site was cutaneous (50.0%), followed by breast (10.3%) and liver (8.6%). Metastatic disease was found at diagnosis in 18 (31.0%) patients, while a known risk factor, such as prior radiotherapy or a clinical syndrome, was present in 14 cases (24.1%).

On light microscopic examination, GC were observed in 24 out of 58 patient samples (41.4%). GC were identified across tumor samples of varying origin, including both cutaneous (13 of 29 samples, 44.8%) and non-cutaneous (11 of 29 samples, 37.9%) subtypes. Despite their frequent occurrence in tumor samples, GC were rare within each sample, frequently comprising less than 1% of the entire tumor cell population examined (Figure 4A). In multivariable analysis, GC were more common in men (odds ratio [OR] 10.46, 95% confidence [CI] 2.46-44.4,  $P = 0.0015$ ), and were associated with high mitotic scores (OR 4.31, 95% CI 1.04-17.8,  $P = 0.0437$ ). Age, ECOG performance status, ethnicity, tumor site, tumor necrosis, presence of epithelioid component,

presence of metastasis at diagnosis, and presence of known risk factors were not significantly correlated (Table 1).

### 3.5 | Survival analysis and response to chemotherapy

We examined the response to chemotherapy in relation to GC status in 27 patients. Compared to those without GC, the presence of GC was associated with a lower rate of objective response (25.0% vs 73.3%,  $P = 0.0213$ ) to either paclitaxel ( $n = 21$ ) or doxorubicin ( $n = 6$ ). Subgroup analysis of the 21 patients who received paclitaxel also revealed poorer response in the GC-positive group (33.3% vs 83.3%,  $P = 0.0318$ ) (Figure 4B).

Furthermore, presence of GC at diagnosis were significantly associated with poorer survival outcomes. Presence of GC was independently associated with poorer OS (median 0.8 vs 1.7 years; HR 2.20, 95% CI 1.17-4.15,  $P = 0.0142$ ) and CSS (median 0.9 vs 1.7 years; HR 2.18, 95% CI 1.12-4.22,  $P = 0.0212$ ) (Figure 4C). Other clinicopathologic factors were examined. While FNCLCC grading is not formally recommended for angiosarcoma, in our cohort, higher FNCLCC grade was also independently associated with poorer OS (0.8 vs 1.4 vs 3.3 years; HR 1.53, 95% CI 1.02-2.30,  $P = 0.0377$ ) and PFS (median 0.4 vs 0.5 vs 2.2 years; HR 2.08, 95% CI 1.38-3.12,  $P = 0.0004$ ). Presence of metastatic disease at diagnosis was independently associated with poorer CSS (median 0.6 vs 1.2 years; HR 2.17, 95% CI 1.11-4.25,  $P = 0.0235$ ), while age >65 at diagnosis was associated with poorer PFS (median 0.6 vs 0.4 years, HR 2.42, 95% CI 1.31-4.46,  $P = 0.0045$ ) (Tables 2-3). Other clinicopathological factors examined were sex, ECOG performance status, ethnicity, tumor site, tumor necrosis, presence of epithelioid component, high mitotic scores, and presence of underlying risk factors, which were found to have no significant correlation with survival outcomes in this cohort.

Age, ECOG performance status, ethnicity, tumor site, tumor necrosis, presence of epithelioid component, presence of metastasis at diagnosis, and presence of known risk factors were not significantly correlated.

TABLE 2 Univariate survival analysis

Characteristic	Overall survival		Progression-free survival		Cancer-specific survival	
	HR (95% CI)	P	HR (95% CI)	P	HR (95% CI)	P
Age at diagnosis (>65 vs ≤65 y)	1.48 (0.79-2.77)	.2171	1.79 (1.08-3.94)	<b>.0291</b>	1.31 (0.68-2.61)	.4025
ECOG performance status (1-4 vs 0)	1.61 (0.90-3.38)	.0994	1.33 (0.73-2.69)	.3051	1.84 (0.99-4.03)	.0528
Ethnicity (Chinese vs non-Chinese)	1.25 (0.51-3.03)	.5147	1.14 (0.48-2.75)	.7478	1.07 (0.42-2.77)	.8859
Giant cell (present vs absent)	<b>2.35 (1.48-5.67)</b>	<b>.0020</b>	2.14 (1.36-5.16)	<b>.0041</b>	<b>2.04 (1.15-4.93)</b>	<b>.0198</b>
Metastasis at diagnosis (present vs absent)	1.74 (0.95-4.33)	.0684	1.59 (0.88-3.85)	.1041	<b>2.08 (1.14-5.61)</b>	<b>.0225</b>
Known risk factor (present vs absent)	0.60 (0.30-1.16)	.1291	0.71 (0.35-1.35)	.2700	0.72 (0.35-1.49)	.3792
Sex (male vs female)	1.38 (0.76-2.64)	.2681	1.54 (0.88-3.00)	.1200	1.09 (0.56-2.15)	.7780
Tumor site (cutaneous vs non-cutaneous)	1.18 (0.64-2.22)	.5698	1.53 (0.88-3.03)	.1175	0.98 (0.50-1.91)	.9544
Tumor grade (high vs intermediate vs low)	<b>1.68 (1.13-2.51)</b>	<b>.0105</b>	<b>1.80 (1.23-2.64)</b>	<b>.0025</b>	1.62 (1.06-2.47)	<b>.0265</b>

CI, confidence interval; ECOG, Eastern Cooperative Oncology Group; HR, hazard ratio.

Bold indicates statistical significant  $P$  values.

**TABLE 3** Cox proportional hazards regression analysis (multivariate analysis)

Characteristic	Overall survival		Progression-free survival		Cancer-specific survival	
	HR (95% CI)	P	HR (95% CI)	P	HR (95% CI)	P
Age at diagnosis (>65 vs ≤65 y)	–	–	2.42 (1.31-4.46)	<b>.0045</b>	–	–
Giant cell (present vs absent)	<b>2.20 (1.17-4.15)</b>	<b>.0142</b>	–	–	2.18 (1.12-4.22)	<b>.0212</b>
Metastasis at diagnosis (present vs absent)	–	–	–	–	2.17 (1.11-4.25)	<b>.0235</b>
Tumor grade (high vs intermediate vs low)	1.53 (1.02-2.30)	<b>.0377</b>	2.08 (1.38-3.12)	<b>.0004</b>	–	–

CI, confidence interval; HR, hazard ratio

Bold indicates statistical significant *P* values.

Giant cells were examined as an additional component to a proposed modified FNCLCC grading system, in which all tumors with GC were considered high grade. Adjustment of grade for GC presence upgraded 4 low grade and eight intermediate grade patients to high grade status and resulted in greater discrimination between survival outcomes of low, intermediate, and high grade groups (Figure 4D-F).

### 3.6 | Nanostring PanCancer IO 360 gene expression analysis

Numerous genes in our analysis were differentially expressed between GC-containing and GC-negative tumors ( $n = 67$  for adjusted  $P < 0.05$ ,  $n = 9$  for adjusted  $P < 0.01$ ) despite adjustment for multiple comparisons (Benjamini-Hochberg). Genes that were significantly overexpressed (adjusted  $P < 0.01$ ) included *COL11A1*, *STC1*, *ERO1A*, *NRAS*, *SAMD9*, and *TWF1*. *COL11A1* expression was increased tenfold in GC-containing tumors, while expression of *STC1* and *ERO1A* were increased sixfold and threefold, respectively. Conversely, *NEIL1*, *C5* and *C7* were significantly underexpressed (adjusted  $P < 0.01$ ) in GC-containing tumors (Figure 5A).

Pathway analysis showed that expression of immune-related metabolic stress and metastasis/matrix remodeling pathways were upregulated in GC-containing tumors. In particular, the enhanced immune-related pathways included cytokine/chemokine signaling, costimulatory signaling, immune cell adhesion/migration, antigen presentation, and cytotoxicity-related pathways. In contrast, in GC-negative tumors, upregulated pathways include NK-kappaB, Notch, Hedgehog, and Wnt signaling pathways, as well as DNA-damage repair and autophagy pathways (Figure 5B). Cell-type analysis of GC-containing tumors was suggestive of enrichment of myeloid cells (neutrophils and macrophages) as well as cytotoxic T cells, while GC-negative tumors contained a larger population of mast cells, NK cells, and TH1-related cells (Figure 5C).

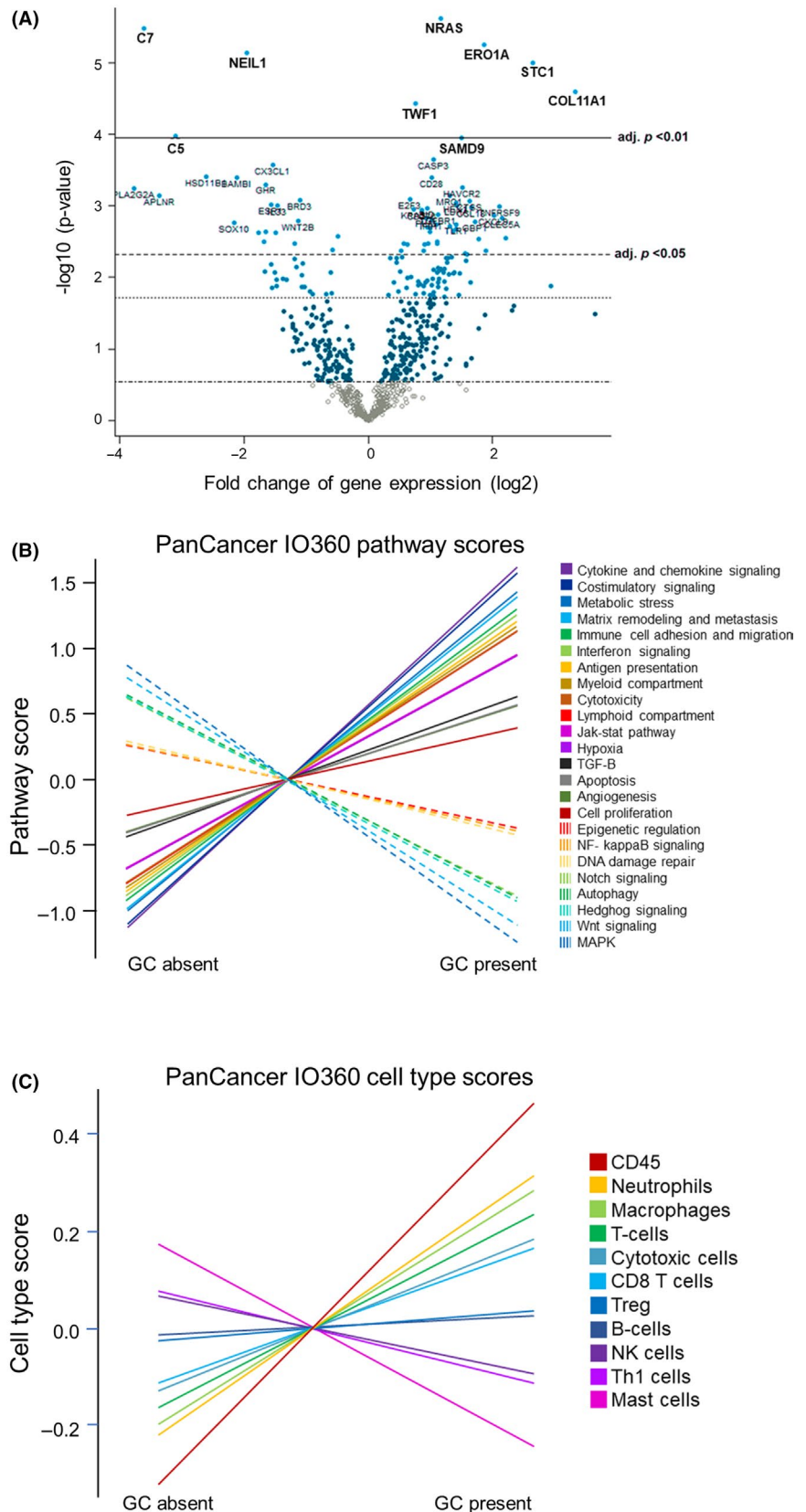
## 4 | DISCUSSION

Our study demonstrated that GC are found in a significant proportion of primary angiosarcoma tumors and also in angiosarcoma cell

lines. We observed that angiosarcoma GC are endothelial in origin and share similarities in genomic profiles to regular-sized cells. Similarly to GC described in other tumor types, they are non-senescent in nature and exhibit mitotic activity, possibly harboring the potential to generate tumorigenic daughter cells via depolyploidization processes such as budding and bursting.<sup>23</sup> While GC have been described in various malignancies, to our knowledge, this is the first study to characterize GC in angiosarcoma and to examine their impact on patient survival. Interestingly, we observed that the presence of GC in primary angiosarcoma tumors was independently associated with poorer patient survival outcomes, along with the presence of distant metastasis, a well-established prognostic factor. While FNCLCC grading has not been recommended for angiosarcoma, we found that FNCLCC grading was prognostic in our patient population and that prognostication via FNCLCC grading could possibly be further refined by integration of GC as a key feature of high-grade disease. This suggests that GC may represent a manifestation of high-grade disease within a continuous spectrum in their histomorphological progression.

Giant cells are thought to contribute to treatment resistance.<sup>6,24</sup> In our study, exposure of ISOHAS and MOLAS cell lines to conventional chemotherapeutic agents paclitaxel and doxorubicin demonstrated that while the majority of the cells exposed to the cytotoxic drugs were eliminated, viable GC were observed at the end of our experiment, and constituted the majority of remaining viable cells. This may reflect the relative chemoresistance of GC in the original culture, or GC formation by regular angiosarcoma cells in response to cytotoxic exposure, which then remained viable despite continued exposure to cytotoxic drugs. In patients with angiosarcoma undergoing chemotherapy, we found that tumors harboring GC were significantly associated with chemoresistance and less likely to respond to therapy, in keeping with our *in vitro* observations. Similarly, a previous preclinical study of GC in colorectal cancer<sup>24</sup> demonstrated findings of GC-driven disease relapse after an appropriate primary treatment response. This study used a mouse model to demonstrate GC-driven regeneration of colon carcinoma tumors after treatment with cisplatin. Intraperitoneal injection of cisplatin resulted in gradual tumor shrinkage and an enrichment of cell population for GC, with subsequent tumor regrowth after a significant delay of

**FIGURE 5** Nanostring PanCancer IO 360 Gene expression analysis. A, Volcano plot illustrating differential expression of selected immuno-oncology-related genes, with comparison between expression in giant cell (GC)- positive and negative tumors. Significant genes with adjusted  $P$ -value  $< 0.01$  are highlighted. B, PanCancer IO 360 pathway scores, illustrating differences in gene expression of selected pathways between GC-positive and negative tumors. C, PanCancer IO 360 cell-type scores, comparing immunologic profiles between GC-positive and negative tumors



approximately 35 days. Notably, regenerated tumor cells were resistant to cisplatin. A more recent study by Coward et al demonstrated possible mechanisms through which polyploid cancer cells may contribute to increased treatment resistance and heterogeneity.

Increased genetic material resulted in slower cell cycling, altered DNA-damage response, and facilitated the generation of new oncogenic mutations. The authors also explored potential treatment targets and proposed possible agents, such as aspirin and resveratrol.<sup>25</sup>

NanoString gene expression profiling revealed significant differences between GC-containing and GC-negative tumors. Of interest, *COL11A1*, *STC1*, and *ERO1a* were significantly overexpressed in GC-containing tumors. *COL11A1*, *STC1*, and *ERO1a* overexpression have been found to be independent poor prognostic factors in a variety of tumor types, including non-small cell lung cancer,<sup>26</sup> esophageal SCC,<sup>27,28</sup> ovarian cancer,<sup>9</sup> and breast cancer.<sup>29,30</sup> Notably, it has also previously been shown that *STC1* (a secreted oncogene in ovarian cancer) is overexpressed in PGCC derived from ovarian cancer cell lines HEY and SKOV3.<sup>31</sup> The upregulation of these genes contributing to poor prognosis in GC-containing tumors is in keeping with our finding of significantly poorer survival in GC-positive patients. The underlying mechanism of this effect, as well as whether upregulation of these genes is confined to GC or seen throughout GC-positive tumors, should be explored in future work. Promisingly, *COL11A1* and *ERO1a* are being explored as therapeutic targets in view of their specificity for malignant cells in multiple tumor types.<sup>32</sup> Development of such therapies may benefit patients with GC-positive angiosarcoma, who currently face limited treatment options and a dismal prognosis. At a pathway level, GC-containing tumors were associated with increased expression of immune-related pathways, metastasis/matrix remodeling pathways, and metabolic stress pathways. Once again, the upregulation of matrix remodeling pathways, which may contribute to invasion and cancer progression, and metastasis pathways is in keeping with the observed poor survival in GC-positive patients.

Our study is limited by its retrospective nature. As archival samples were used for determination of GC presence, there was potential for sampling error. Samples included both core biopsy and surgically obtained specimens, of which there was variation in sample size depending on original sample collection methods. Nonetheless, we provided an initial characterization for the malignant nature of GC in angiosarcomas and elucidated their potential clinical significance. Further studies to characterize GC in angiosarcoma will be needed to confirm their contribution to treatment resistance and survival outcomes.

## ACKNOWLEDGMENTS

This work was supported by the Singapore Ministry of Health's National Medical Research Council of Singapore NMRC/FLWSHP/054/2017-00 and NMRC/CG/C012B/2017\_NCCS, MOH-STAR18NOV-0001, SHF-Foundation (SHF/FG653P/2017) as well as the SingHealth Duke-NUS Academic Medical Centre and Oncology ACP (08-FY2017/P1/14-A28). We would like to thank all subjects who participated in this study.

## DISCLOSURE

The authors declare no competing financial interests.

## ORCID

Grace Fangmin Tan  <https://orcid.org/0000-0002-3910-1509>

Jason Yongsheng Chan  <https://orcid.org/0000-0002-4801-3703>

## REFERENCES

- White-Gilbertson S, Voelkel-Johnson C. Giants and monsters: Unexpected characters in the story of cancer recurrence. *Adv Cancer Res.* 2020;148:201-232.
- Zhang D, Yang X, Yang Z, et al. Daughter cells and erythroid cells budding from PGCCs and their clinicopathological significances in colorectal cancer. *J Cancer.* 2017;8:469-478.
- Zhang L, Ding P, Lv H, et al. Number of polyploid giant cancer cells and expression of EZH2 are associated with VM formation and tumor grade in human ovarian tumor. *Biomed Res Int.* 2014;2014:903542.
- Lv H, Shi Y, Zhang L, et al. Polyploid giant cancer cells with budding and the expression of cyclin E, S-phase kinase-associated protein 2, stathmin associated with the grading and metastasis in serous ovarian tumor. *BMC Cancer.* 2014;14:576.
- Fei F, Zhang D, Yang Z, et al. The number of polyploid giant cancer cells and epithelial-mesenchymal transition-related proteins are associated with invasion and metastasis in human breast cancer. *J Exp Clin Cancer Res.* 2015;34:158.
- Mirzayans R, Andrais B, Murray D. Roles of polyploid/multinucleated giant cancer cells in metastasis and disease relapse following anticancer treatment. *Cancers (Basel).* 2018;10:118.
- Amend SR, Torga G, Lin KC, et al. Polyploid giant cancer cells: unrecognized actuators of tumorigenesis, metastasis, and resistance. *Prostate.* 2019;79:1489-1497.
- Pundalikappa SS, Channaveerappa HB, Theresa SM, Venkatesh BR. Dedifferentiated liposarcoma of thigh: tumor with monster cells. *Clin Cancer Investig J.* 2016;5:188-192.
- Erenpreisa JA, Cragg MS, Fringes B, Sharakhov I, Illidge TM. Release of mitotic descendants by giant cells from irradiated Burkitt's lymphoma cell lines. *Cell Biol Int.* 2000;24:635-648.
- Dome JS, Cotton CA, Perlman EJ, et al. Treatment of anaplastic histology Wilms' tumor: results from the fifth National Wilms' Tumor Study. *J Clin Oncol.* 2006;24:2352-2358.
- Fayette J, Martin E, Piperno-Neumann S, et al. Angiosarcomas, a heterogeneous group of sarcomas with specific behavior depending on primary site: a retrospective study of 161 cases. *Ann Oncol.* 2007;18:2030-2036.
- Young RJ, Brown NJ, Reed MW, Hughes D, Woll PJ. Angiosarcoma. *Lancet Oncol.* 2010;11:983-991.
- Chan JY, Lim JQ, Yeong J, et al. Multi-omic analysis and immunoprofiling reveals distinct subtypes of human angiosarcoma. *J Clin Invest.* 2020;130(11):5833-5846.
- Ragavan S, Lim HJ, Tan JW, et al. Axillary lymph node dissection in angiosarcomas of the breast: an Asian institutional perspective. *Sarcoma.* 2020;2020:4890803.
- Penel N, Italiano A, Ray-Coquard I, et al. Metastatic angiosarcomas: doxorubicin-based regimens, weekly paclitaxel and metastasectomy significantly improve the outcome. *Ann Oncol.* 2012;23:517-523.
- Chan JY, Zhang Z, Chew W, et al. Biological significance and prognostic relevance of peripheral blood neutrophil-to-lymphocyte ratio in soft tissue sarcoma. *Sci Rep.* 2018;8:11959.
- Layfield LJ, Fanning T. *Cytopathology of Bone and Soft Tissue Tumors.* Oxford: Oxford University Press; 2002.
- Nawar NA, Olsen J, Jelic TM, He C. Primary urinary bladder angiosarcoma with osteoclast-like multinucleated giant cells: a case report and literature review. *Am J Case Rep.* 2016;17:143-149.
- Guillou L, Coindre J-M, Bonichon F, et al. Comparative study of the National Cancer Institute and French Federation of Cancer Centers Sarcoma Group grading systems in a population of 410 adult patients with soft tissue sarcoma. *J Clin Oncol.* 1997;15:350-362.
- Li H, Durbin R. Fast and accurate short read alignment with Burrows-Wheeler transform. *Bioinformatics.* 2009;25:1754-1760.

21. Adalsteinsson VA, Ha G, Freeman SS, et al. Scalable whole-exome sequencing of cell-free DNA reveals high concordance with metastatic tumors. *Nat Commun.* 2017;8:1324.
22. Eisenhauer EA, Therasse P, Bogaerts J, et al. New response evaluation criteria in solid tumours: revised RECIST guideline (version 1.1). *Eur J Cancer.* 2009;45:228-247.
23. Zhang S, Mercado-Uribe I, Xing Z, Sun B, Kuang J, Liu J. Generation of cancer stem-like cells through the formation of polyploid giant cancer cells. *Oncogene.* 2014;33:116-128.
24. Puig PE, Guilly MN, Bouchot A, et al. Tumor cells can escape DNA-damaging cisplatin through DNA endoreduplication and reversible polyploidy. *Cell Biol Int.* 2008;32:1031-1043.
25. Coward J, Harding A. Size does matter: why polyploid tumor cells are critical drug targets in the war on cancer. *Front Oncol.* 2014;4:123.
26. Shen L, Yang M, Lin Q, Zhang Z, Zhu B, Miao C. COL11A1 is over-expressed in recurrent non-small cell lung cancer and promotes cell proliferation, migration, invasion and drug resistance. *Oncol Rep.* 2016;36:877-885.
27. Shirakawa M, Fujiwara Y, Sugita Y, et al. Assessment of stanniocalcin-1 as a prognostic marker in human esophageal squamous cell carcinoma. *Oncol Rep.* 2012;27:940-946.
28. Zhang B, Zhang C, Yang X, et al. Cytoplasmic collagen XI $\alpha$ 1 as a prognostic biomarker in esophageal squamous cell carcinoma. *Cancer Biol Ther.* 2018;19:364-372.
29. Wu YH, Chang TH, Huang YF, Huang HD, Chou CY. COL11A1 promotes tumor progression and predicts poor clinical outcome in ovarian cancer. *Oncogene.* 2014;33:3432-3440.
30. Kutomi G, Tamura Y, Tanaka T, et al. Human endoplasmic reticulum oxidoreductin 1- $\alpha$  is a novel predictor for poor prognosis of breast cancer. *Cancer Sci.* 2013;104:1091-1096.
31. Zhang S, Mercado-Uribe I, Hanash S, Liu J. iTRAQ-based proteomic analysis of polyploid giant cancer cells and budding progeny cells reveals several distinct pathways for ovarian cancer development. *PLoS One.* 2013;8:e80120.
32. Jia D, Liu Z, Deng N, et al. A COL11A1-correlated pan-cancer gene signature of activated fibroblasts for the prioritization of therapeutic targets. *Cancer Lett.* 2016;382:203-214.

**How to cite this article:** Tan GF, Goh S, Lim AH, et al. Bizarre giant cells in human angiosarcoma exhibit chemoresistance and contribute to poor survival outcomes. *Cancer Sci.* 2021;112:397-409. <https://doi.org/10.1111/cas.14726>